

# Formation of calcium deficient hydroxyapatite at near-physiological temperature

M. T. FULMER, R. I. MARTIN, P. W. BROWN

Materials Research Laboratory, University Park, PA 16802, USA

The formation of calcium deficient hydroxyapatite  $\text{Ca}_9(\text{HPO}_4)(\text{PO}_4)_5\text{OH}$  (HAp) at 25 °C by reaction of tetracalcium phosphate (TetCP), monocalcium phosphate monohydrate (MCPM), and calcium hydroxide was investigated. Phase pure, calcium deficient hydroxyapatite was prepared in approximately 3.25 h at 25 °C by the reaction of dilute suspensions. Variations in the solution pH, calcium, and phosphorus concentration were determined during the reactions. The solution conditions for all reactions investigated show similar behaviour. Isothermal calorimetry was carried out to determine the rates of heat evolution during reaction. Results indicate that significant reaction occurs in the first 15 min. During this period the solution pH ranges from 4.5 to 7.5 during three distinct stages of reaction. Early reaction occurs at low pH due to rapid MCPM dissolution. The presence of  $\text{Ca}(\text{OH})_2$  effects the pH in the first 2 min of reaction in association with the proportion of MCPM. Brushite ( $\text{CaHPO}_4 \cdot 2\text{H}_2\text{O}$ ) is the predominant product formed until MCPM is consumed. X-ray diffraction analysis confirmed that brushite formed as an intermediate in the first few minutes. Brushite precipitated as thin plates having varying geometric shapes. A second stage is the reaction of brushite, tetracalcium phosphate, and  $\text{Ca}(\text{OH})_2$  (if present) as the solution adjusts to invariant conditions while forming hydroxyapatite. A rise in pH occurs during this period. A third stage of reaction proceeds at relatively constant near-physiological pH conditions for the remainder of the reaction as brushite is consumed along with tetracalcium phosphate in forming hydroxyapatite.

## 1. Introduction

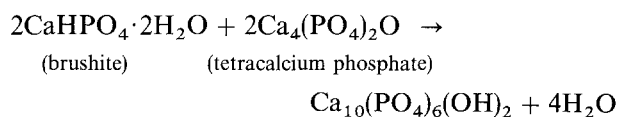
Hard vertebrate tissues are composites primarily composed of impure, calcium deficient hydroxyapatite and collagen. The formula for stoichiometric hydroxyapatite is  $\text{Ca}_{10}(\text{PO}_4)_6(\text{OH})_2$ . However, this compound exists over a range of compositions that may be characterized in terms of Ca/P ratios. The Ca/P ratio of stoichiometric material is 1.67. Stable compositions may have Ca/P ratios extending to approximately 1.5,  $\text{Ca}_9(\text{HPO}_4)(\text{PO}_4)_5\text{OH}$  assuming that no ionic substitution has taken place in the apatite structure. The latter is calcium deficient HAp, which is a defective structure created by the removal of a mole of CaO from the stoichiometric HAp.

The biocompatibility of hydroxyapatite makes it attractive for use in medical devices. Applications involving such uses of hydroxyapatite are widespread, and range from drug delivery systems to orthopaedic devices. Further, apatitic materials have found use for applications involving both orthopaedics [1–3] and dentistry [4, 5]. There is, in addition, interest in coating the surfaces of metallic prostheses with hydroxyapatite as a means to promote bone intergrowth, and thereby improving the bond between bone and prosthesis [6, 7]. However, little appears to have been published with respect to the identification

of suitable means to allow the formation of hydroxyapatite *in vivo*. Therefore, it is the object of this study to investigate the low-temperature formation of hydroxyapatite.

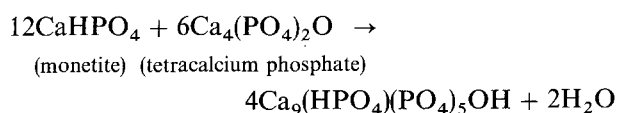
Much work has been done to investigate hydroxyapatite precipitation. For example, studies of the precipitation of hydroxyapatite or its precursor phases have been carried out at low supersaturation [8, 9], moderate supersaturation [10], and high supersaturation [11]. In these investigations, hydroxyapatite (or its precursors) was precipitated from solutions of soluble salts such as  $\text{Na}_2\text{HPO}_4$  and  $\text{CaCl}_2$ . A consequence of forming calcium phosphates by the reaction of salts is that the processes of nucleation and growth are not occurring under steady-state conditions. In addition, calcium phosphate formation always occurs in the presence of neutral electrolytes. Recognizing this, Nancollas and coworkers investigated the formation of hydroxyapatite at constant composition [12, 13]. In these studies, reactants are continuously added to the system to maintain constant reaction conditions. Constant composition studies provide superior kinetic information while being the most simulative of conditions *in vivo*. More recently it was discovered [14] that it is possible to form stoichiometric hydroxyapatite at low temperature by the

following reaction:



Under ideal conditions, dissolution of the reactants drives the solution composition to an invariant point which is the intersection of the solubility curves for these two reactants. The solution at this metastable invariant point is supersaturated with respect to hydroxyapatite which precipitates. Continuing dissolution of the reactants continues to supply calcium and phosphate ions to solution while continued hydroxyapatite formation depletes the solution of these ions. If hydroxyapatite formation occurs under these conditions, it will precipitate from a solution whose pH is approximately 7.4. This is the pH value observed for physiological extracellular fluids [15]. Thus, Brown and Chow [14] demonstrated an ambient temperature process by which stoichiometric hydroxyapatite can be made. However, bone apatite is calcium deficient. Calcium deficiency of bone apatite has significant implications affecting its ability to remodel. Comparison of the solubility products of stoichiometric and calcium deficient hydroxyapatite provides a qualitative indication of the relative propensities of the two apatites to be resorbed. Based on the comparison of solubility products [16], calcium deficient hydroxyapatite is approximately 22 orders of magnitude more soluble than stoichiometric hydroxyapatite.

Previously, we investigated the formation of calcium deficient HAp using the following reaction [17]:



We observed that a steady-state condition [18] is

rapidly attained. However, the solution pH during hydroxyapatite formation was always higher than that of the invariant point between  $\text{CaHPO}_4$  and  $\text{Ca}_4(\text{PO}_4)_2\text{O}$ . This indicates that the dissolution of the acidic phase monetite,  $\text{CaHPO}_4$ , is rate limiting. In the present study we have used  $\text{Ca}(\text{H}_2\text{PO}_4)_2 \cdot \text{H}_2\text{O}$ , a reactant more acidic, and soluble than  $\text{CaHPO}_4$ , and investigate the variations in solution chemistry and the kinetics of hydroxyapatite formation.

## 2. Materials and methods

Three reactants, tetracalcium phosphate (TetCP) ( $\text{Ca}_4(\text{PO}_4)_2\text{O}$ ), monocalcium phosphate monohydrate (MCPM) ( $\text{Ca}(\text{H}_2\text{PO}_4)_2 \cdot \text{H}_2\text{O}$ ), and calcium hydroxide were dry mixed in different molar ratios to obtain a constant Ca/P ratio of 1.5. Table II lists the formula units, names, and acronyms of the phases discussed as a reference point. The six reactions studied are shown in Table I with theoretical products. The molar ratio of the reactant  $\text{Ca}(\text{OH})_2$  to the product HAp was varied between 0 and 3. TetCP was prepared in our laboratory and milled to a mean particle diameter of 1.3  $\mu\text{m}$ . Reagent grade MCPM, and  $\text{Ca}(\text{OH})_2$  were obtained commercially. The mean diameter of the  $\text{Ca}(\text{OH})_2$  is 12  $\mu\text{m}$ . The average size of MCPM crystals was not measured.

Calcium and phosphate concentrations and pH were measured during reaction of dilute suspensions having a liquid-to-solids ratio of 100 at 25 °C. At predetermined intervals during the reactions, 10 ml of solution containing both solids and liquids were drawn out via disposable syringes, and injected through 0.2  $\mu\text{m}$  millipore filters. The filtered solutions were analysed for calcium and phosphate concentrations by DC plasma atomic emission spectroscopy. In addition to solution chemistry determinations, small amounts of solids were extracted from the solutions at various times by filtering through a Büchner funnel with Whatman 540 filter paper. Further reactions of

TABLE I The reactions investigated

		$\text{Ca}(\text{OH})_2$ TetCP	$\text{Ca}(\text{OH})_2$ HAp
(1)	$1\text{Ca}(\text{H}_2\text{PO}_4)_2 \cdot \text{H}_2\text{O} + 2\text{Ca}_4(\text{PO}_4)_2\text{O} = \text{HAp} + 2\text{H}_2\text{O}$	0.000	0.00
(2)	$13\text{Ca}(\text{H}_2\text{PO}_4)_2 \cdot \text{H}_2\text{O} + 23\text{Ca}_4(\text{PO}_4)_2\text{O} + 3\text{Ca}(\text{OH})_2 = 12\text{HAp} + 30\text{H}_2\text{O}$	0.131	0.25
(3)	$7\text{Ca}(\text{H}_2\text{PO}_4)_2 \cdot \text{H}_2\text{O} + 11\text{Ca}_4(\text{PO}_4)_2\text{O} + 3\text{Ca}(\text{OH})_2 = 6\text{HAp} + 18\text{H}_2\text{O}$	0.272	0.50
(4)	$4\text{Ca}(\text{H}_2\text{PO}_4)_2 \cdot \text{H}_2\text{O} + 5\text{Ca}_4(\text{PO}_4)_2\text{O} + 3\text{Ca}(\text{OH})_2 = 3\text{HAp} + 12\text{H}_2\text{O}$	0.600	1.00
(5)	$5\text{Ca}(\text{H}_2\text{PO}_4)_2 \cdot \text{H}_2\text{O} + 4\text{Ca}_4(\text{PO}_4)_2\text{O} + 6\text{Ca}(\text{OH})_2 = 3\text{HAp} + 18\text{H}_2\text{O}$	1.500	2.00
(6)	$2\text{Ca}(\text{H}_2\text{PO}_4)_2 \cdot \text{H}_2\text{O} + \text{Ca}_4(\text{PO}_4)_2\text{O} + 3\text{Ca}(\text{OH})_2 = \text{HAp} + 8\text{H}_2\text{O}$	3.000	3.00

HAp =  $\text{Ca}_9(\text{HPO}_4)(\text{PO}_4)_5\text{OH}$

TABLE II Reference list for the phases described

Acronym	Name	Formula unit
MCPM	Monocalcium phosphate monohydrate	$\text{Ca}(\text{H}_2\text{PO}_4)_2 \cdot \text{H}_2\text{O}$
TetCP	Tetracalcium phosphate	$\text{Ca}_4(\text{PO}_4)_2\text{O}$
HAp	Hydroxyapatite	$\text{Ca}_{10-x}(\text{HPO}_4)_x(\text{PO}_4)_{6-x}(\text{OH})_{2-x}$
DCPD	Brushite	$\text{CaHPO}_4 \cdot 2\text{H}_2\text{O}$
DCP	Monetite	$\text{CaHPO}_4$

the harvested solids were quenched in acetone. Powder X-ray diffraction data was obtained on a Scintag automated diffractometer between  $4^\circ$  and  $56^\circ$  ( $2\theta$ ).

Heats of reaction,  $\Delta H_r$ , were measured by isothermal calorimetry. In this method heat liberated as a result of exothermic reactions is detected by thermopiles which surround the reacting sample. By using a calibration constant the voltage output from the thermopiles can be converted to a thermal output and the heat of reaction  $\Delta H_r$  is thereby determined. The liquid-to-solids ratio used in the calorimetric experiments was 1:1. The amounts of each reactant were adjusted to yield a constant weight of calcium deficient HAp product at complete reaction. The powders were dry mixed in the various proportions shown in Table I, placed in gold-plated copper sample cups, and equilibrated at  $25^\circ\text{C}$  along with the liquid reactant. Once equilibration was attained, the liquid was injected into the reactant powders, and the rates of heat liberation monitored by a computer system. Integration of the rate data yields the total heat evolved as a function of time during the reaction.

An Electroscan environmental scanning electron microscope (ESEM) was used to study the morphologies of the products formed. This SEM allows the morphologies of samples to be observed without the need for conductive coatings. The charge accumulated on the surface of the sample is bled off by the water vapour pressure that is adjusted within the specimen chamber. Therefore, non-conductive surfaces can be observed with this SEM.

### 3. Results and discussion

#### 3.1. Solution chemistry

A plot comparing the variations in pH values during the first 24 h of reaction at liquid-to-solids ratio of 100 for the six reactions listed in Table I is shown in Fig. 1. The same trend is observed in all cases. The initial pH (1 min after mixing) is directly correlated to the amount of  $\text{Ca}(\text{OH})_2$  present. However, after the first 2 min of reaction there is no further correlation. The solution pH is observed to increase slowly during the

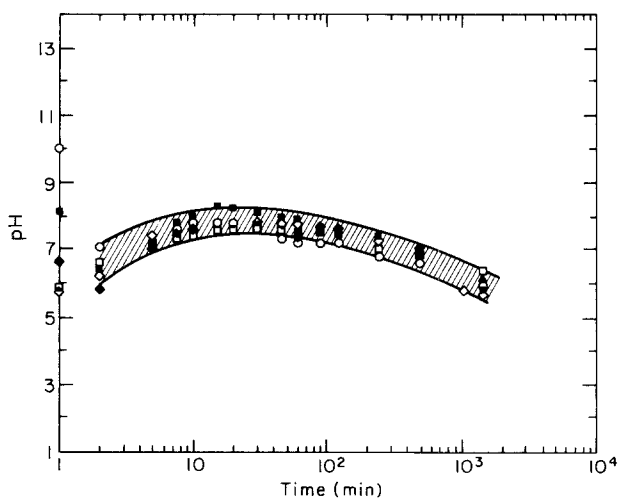
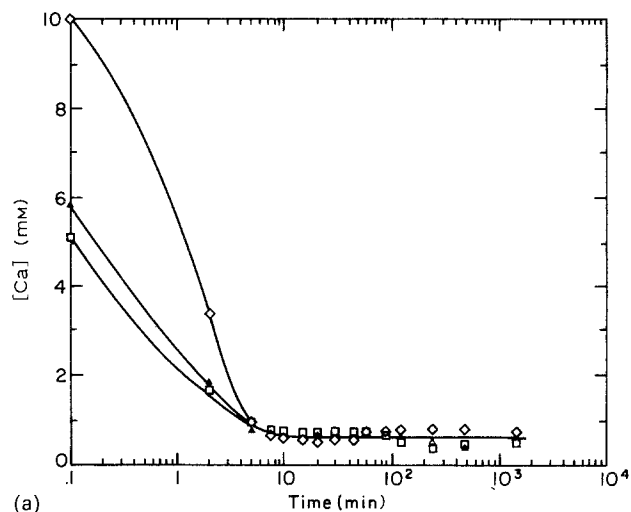


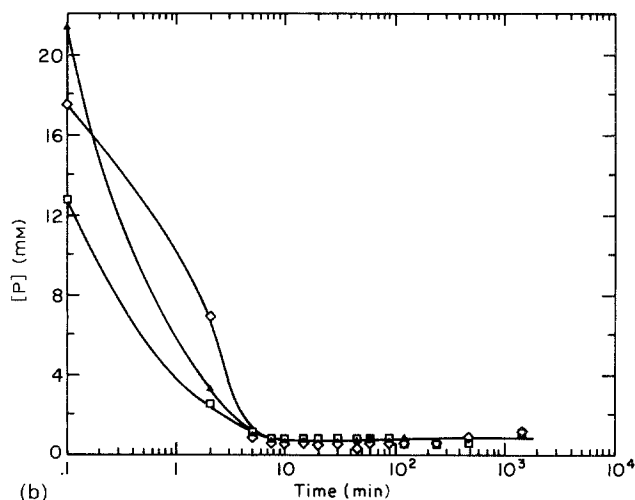
Figure 1 The variations in solution pH during the first 24 h for the reactions listed in Table I. Similar behaviour is observed. Reactions: 1 ( $\square$ ), 2 ( $\blacklozenge$ ), 3 ( $\blacktriangle$ ), 4 ( $\diamond$ ), 5 ( $\blacksquare$ ), 6 ( $\circ$ ).

period between 2 and 20 min reaching a value somewhat below pH 8. Between 20 min and 24 h the solution pH slowly decreases to a value near 6. The initial drop in the solution pH shown in Fig. 1 indicates rapid MCPM dissolution, and it was confirmed by X-ray diffraction analysis that MCPM was no longer detectable 2 min after hydration.

Calcium and phosphate concentrations were determined at a liquid-to-solids ratio of 100 for three of the reactions listed in Table I. These reactions involve MCPM, and TetCP in the absence of  $\text{Ca}(\text{OH})_2$ , and at  $\text{Ca}(\text{OH})_2/\text{HAp}$  ratios of 1 and 2 (reactions 1, 4 and 5, respectively). Fig. 2a shows the variation in calcium concentration during these reactions. The same general behaviour is exhibited in all three reactions. During the first 10 min of reaction, the calcium ion concentrations decrease from values that are related to the original fractions of  $\text{Ca}(\text{OH})_2$ , or in other words the initial ratios of the reactants present to a nominally constant value of about 0.6 mM. This steady-state calcium concentration is maintained thereafter. The variations in the total phosphate concentration in solution are shown in Fig. 2b. These variations are very similar to those observed for calcium. The total phosphate concentrations for these reactions are approximately equimolar with the calcium concentration ( $\sim 0.7$  mM) after 10 min.



(a)



(b)

Figure 2 The variations in calcium (a) and phosphate (b) concentration for reaction at  $\text{Ca}(\text{OH})_2/\text{HAp}$  ratios of 0, 1, and 2. Reactions: 1 ( $\square$ ), 4 ( $\blacktriangle$ ), 5 ( $\diamond$ ).

### 3.2. X-ray diffraction analysis

Powder X-ray diffraction was used to determine the phases present at varying times of reaction in the dilute suspensions. Highly crystalline brushite is formed initially, and then becomes a reactant as the pH rises, and dissolution of MCPM and  $\text{Ca}(\text{OH})_2$  are complete. Diffraction analysis carried out after 2 h of reaction in the absence of  $\text{Ca}(\text{OH})_2$  showed that both brushite and HAp had formed, and that TetCP was still present. An X-ray pattern after 24 h of reaction detects only HAp.

The X-ray patterns obtained after about 3 h of reaction in dilute suspension for the reactions in Table I that involve  $\text{Ca}(\text{OH})_2$  all show diffraction peaks from poorly crystalline HAp; brushite is no longer observed. An extensive X-ray study of reaction  $4(\text{Ca}(\text{OH})_2/\text{HAp} = 1)$  was carried out to fully explain the mechanisms of HAp formation, and to determine the time required for complete reaction. Small samples were extracted from solution after times of 0.1, 1, 1.5, 2, 5, and 10 min, and 1–8 h of reaction. Patterns obtained at reaction times of less than 10 min reveal brushite and HAp, along with residual TetCP. The brushite crystallites that form in the initial stages of the reaction are small, thin sheets. This can be seen in Fig. 3 which is an electron micrograph showing the uncoated products formed after 5 min of reaction. The brighter particles in this micrograph have the morphology of unreacted TetCP. The ability to observe the samples without coating shows that extremely thin crystals of brushite are formed. Particles behind the brushite crystals demonstrate the thinness of the crystals.

Analysis of the X-ray diffraction data also indicates that MCPM and  $\text{Ca}(\text{OH})_2$  (if present) are not detectable after 1–2 and 5–10 min of hydration, respectively. Analyses carried out after 1, 2 and 3 h of reaction in dilute suspension show decreasing relative amounts of brushite and increasing amounts of HAp. It was determined that 3.25 h of reaction time were required to form phase pure HAp from dilute suspensions.

The mechanistic path involves the formation of brushite as an intermediate, which is eventually consumed in the formation of HAp. A local equilibrium argument can be used to describe the initial formation of brushite. It has been established [19] that MCPM



Figure 3 The products formed in the first 15 min of reaction at a  $\text{Ca}(\text{OH})_2/\text{HAp}$  ratio of 1.

dissolves incongruently. The incongruent dissolution of MCPM results in the formation of brushite even though the pH is in the range in which HAp is the stable phase. Although HAp is the thermodynamically favoured phase to be formed, brushite is favoured kinetically.

The liquid-to-solids ratio was found to greatly influence the reaction kinetics. The initial stages of reaction are indistinguishable in dilute suspensions. However, three stages are apparent in solution chemistry data obtained at liquid-to-solids ratio of 1.0 in the absence of stirring. The pH variations during the first 15 min of reaction at a liquid-to-solids ratio of 1 are shown in Fig. 4. This ratio was selected because it was also used in the calorimetric experiments which will be discussed. Triplicate determinations of these variations in pH were obtained and the data is reproducible. In one instance the reactants were MCPM and TetCP, while in the second  $\text{Ca}(\text{OH})_2$  was also a reactant (reactions 1 and 4 in Table I). The pH variations for these reactions show the same general behaviour. The general sequence of reactions ultimately leading to the formation of calcium deficient HAp at both dilute suspensions liquid-to-solids ratio of 100, and slurries of high solids content liquid-to-solids ratio of 1 is summarized in Fig. 5.

The magnitudes of the initial variations in pH liquid-to-solids ratio of 1 are related to the initial proportions of the constituents. The initial drop in pH was somewhat greater when one of the reactants is  $\text{Ca}(\text{OH})_2$ . In this instance the proportion of MCPM is relatively larger (weight fraction MCPM = 0.352) than in the case where  $\text{Ca}(\text{OH})_2$  is absent (weight fraction MCPM = 0.256). The observed behaviour indicates that the pH during the initial stages of reaction is dominated by the dissolution of MCPM. The enhanced depression in pH is consistent with the presence of a larger amount of this reactant. The pH reaches a minimum value near 4.6 when  $\text{Ca}(\text{OH})_2$  is present, and a minimum value of 5.2 when it is not.

Companion X-ray diffraction analyses indicate the following sequence of reactions which are in accord

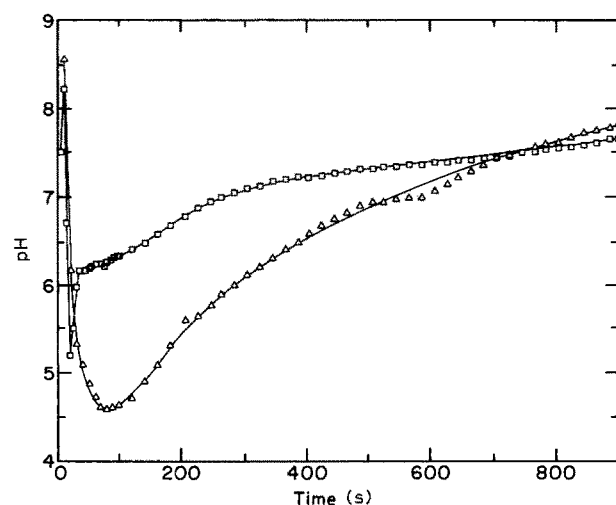


Figure 4 Variations in pH study during the first 15 min after mixing for  $\text{Ca}(\text{OH})_2/\text{HAp}$  ratios of 0 and 1. Three distinct stages of reaction can be observed. After the first 100 s of reaction, only every fourth data point is plotted. Reactions: 1 (□), 4 (△).

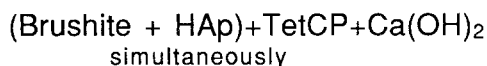
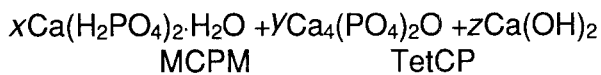


Figure 5 A general sequence of reactions for low and high liquid-to-solids ratios ultimately leading to the formation of calcium deficient HAp.

with HAp formation occurring in three stages. Brushite formation dominates stage I. Reaction 4 (in Fig. 4) levels off at a pH value of 4.6. This pH value corresponds to that of the stable invariant point involving brushite and HAp which is achieved momentarily, suggesting the presence of HAp. The complete dissolution of MCPM marks the end of stage I, and stage II follows. The brushite formed in the early stages of reaction begins to dissolve now that it is the most acidic phase present. However, an increase in pH observed in Fig. 4 implies that the basic phase(s) are dissolving more rapidly than brushite causing the ionic concentrations in solution to adjust to different invariant conditions. Ca(OH)<sub>2</sub> (if present) is completely consumed early in stage II. When Ca(OH)<sub>2</sub> is a reactant, a longer time is required to achieve these invariant conditions due to the depressed pH values achieved in the first few minutes.

At the end of stage II the pH is near neutral in both instances. Stage III is characterized by negligible variations in pH. This behaviour is consistent with a metastable invariant point involving brushite and TetCP having been achieved. The pH values observed in this study after 15 min of reaction are approximately 7.4 in both instances. This value is reported for the metastable invariant point between brushite and TetCP [14]. As was the case for the experiments carried out in dilute suspensions, brushite formation is observed at a pH where HAp is the stable phase. Further, although Ca(OH)<sub>2</sub> did not affect the solution

composition after the first minutes of reaction, its presence was found to increase the amount of brushite observed in the X-ray diffraction patterns after 8 h of reaction for all of the reactions investigated at the liquid-to-solids ratio of 1. This is explained by the increase in MCPM reactant required to form calcium deficient HAp upon increasing Ca(OH)<sub>2</sub> addition. In contrast to a variety of findings suggesting octacalcium phosphate (OCP) Ca<sub>8</sub>H<sub>2</sub>(PO<sub>4</sub>)<sub>6</sub>·5H<sub>2</sub>O as an HAp precursor [20–22], OCP was never observed.

### 3.3. Kinetics of formation

Heat evolution data were obtained at 25 °C for the six different reactions listed in Table I at a liquid-to-solids ratio of 1. Fig. 6 shows a typical calorimetric rate curve obtained in this case during reaction 4 of Table I. Fig. 7 shows the total amount of heat evolved during the reactions listed in Table I, normalized with respect to the moles of TetCP present. A seventh curve showing the total heat evolution during reaction of CaHPO<sub>4</sub> and TetCP is shown for comparison. The curves presented in this figure are obtained by integrating the rate curves.

The data presented in Fig. 7 show an initial period during which significant heat is evolved when MCPM is a reactant. This initial period ends after approximately 15 min regardless of the initial proportions of

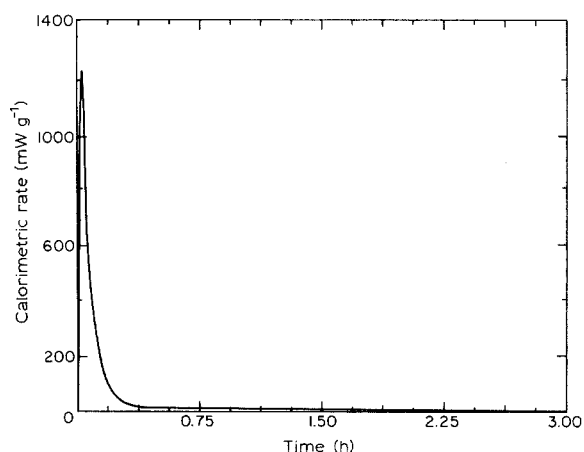


Figure 6 The calorimetric rate curve ( $dQ/dt$ ) obtained at 25 °C when the Ca(OH)<sub>2</sub>/HAp ratio is 1.

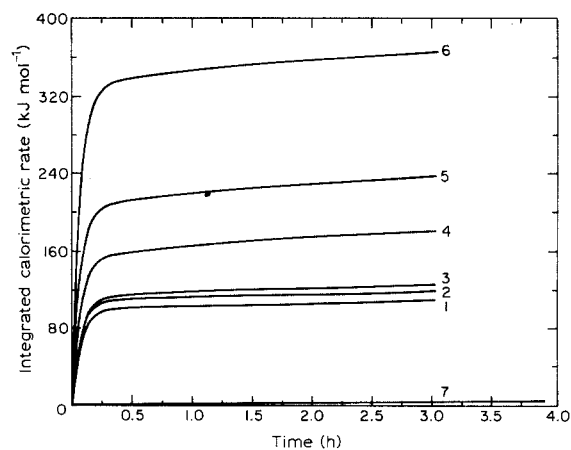


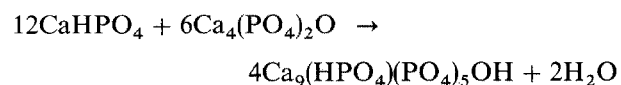
Figure 7 The integrated calorimetric curves for the reactions listed in Table I (curves 1–6), and that from reaction of monetite and tetracalcium phosphate at 25 °C in a molar ratio of 2:1 (curve 7).

constituents used. Qualitative comparison to the heat evolved for complete reaction shows that the reaction is approximately 70% complete after 15 min. While the total heat evolved is compositionally dependent, correlating directly with the amount of  $\text{Ca}(\text{OH})_2$  originally present, the overall kinetic behaviour appears to be independent of the relative proportions of reactants. The variations in solution chemistry leading to the formation of brushite previously described reach completion early in this period. Although the development of mechanical properties was not the objective of this study, and the reaction is still incomplete after 15 min, consolidated and relatively hard masses had formed by this time.

A study was done to determine the time required for the  $\text{Ca}(\text{OH})_2$ , and MCPM present in reaction 4 from Table I, to be consumed. The reactants were hydrated at a liquid-to-solids ratio of 1. After 1 min of reaction, a small quantity of solids was removed from the reaction vessel, and quenched in acetone to stop the reaction. This process was repeated every 15 s for 5 min. The samples were then characterized by X-ray diffraction. The pattern obtained before reaction identified MCPM, TetCP, and very low intensity peaks corresponding to  $\text{Ca}(\text{OH})_2$ . Calcium hydroxide was not easily detectable after 5 min of reaction (due to the high crystallinity of brushite). Duplicate experiments showed the same results, suggesting that the  $\text{Ca}(\text{OH})_2$  reactant has been consumed after about 5 min of reaction.

Returning to Fig. 7, the slopes of the heat evolution curves are independent of composition after the first 15 min of reaction. This indicates that the rates of heat evolution following the first 15 min do not depend on composition. It is during this period of slow reaction that HAp is forming from reaction of brushite and TetCP at steady-state conditions. Fig. 7 also shows that the rate of heat evolution after 3 h of reaction becomes negligible. This length of time coincides with that required in the solution chemistry experiments for dilute suspensions to yield phase pure HAp. The phases present after termination of the calorimetric experiments were identified by X-ray diffraction to be a mixture of brushite, TetCP and HAp even after reaction times of 24 h. This indicates the effects of the two liquid-to-solids ratios used (1 and 100) on the rate of HAp formation.

The heat evolved during the reaction of  $\text{CaHPO}_4$  and TetCP when mixed at a molar ratio of 2:1 is shown as curve 7 in Fig. 7. Complete reaction of these reactants also leads to the formation of calcium deficient HAp, according to:



The heat evolved by this reaction is significantly less than the heat evolved by reactions 1–6 (Table I) over the period of study. X-ray diffraction showed that all reactions involving  $\text{Ca}(\text{OH})_2$  (reaction 2–6) are relatively complete after 3 h. Reaction 1 was also near completion; however, more brushite was observed in X-ray patterns. In contrast the reaction of monetite

and TetCP has been shown [17, 18] to require two weeks to reach completion. This is the result of the onset of a diffusionally controlled reaction due to the overgrowth of HAp on the monetite crystals as a result of the incongruent dissolution of the latter [18]. Such overgrowth was not observed in the present study. In the reactions involving MCPM, the initial formation of brushite is coincident with the formation of HAp. As a consequence brushite does not become covered with an HAp layer as it forms. In addition, the brushite which forms exhibits both a high surface area and a morphology that cannot be obtained by milling. Therefore, the diffusionally controlled rate-limiting reactions that are observed during reaction of monetite with TetCP are minimized leading to the more rapid HAp formation.

#### 4. Conclusions

Analysis of the variations in the aqueous phase during hydroxyapatite formation were carried out by using dilute suspensions (liquid-to-solids ratio of 100), and slurries of high solids content (liquid-to-solids ratio of 1). Phenomenologically, similar behaviour was observed. However, the relative reaction rates are higher in dilute suspensions and reach completion in about 3 h. Qualitative analysis of the heat evolution for reactions at high solids content suggests that 70% of reaction takes place in the first 15 min. Regardless of the experimental conditions, the solution pH rapidly enters a range where HAp is the thermodynamically favoured phase. However, brushite formation occurs in virtually every instance. This indicates the formation of the latter to be kinetically favoured.

Sequentially, MCPM,  $\text{Ca}(\text{OH})_2$  and TetCP react to form brushite and HAp simultaneously, then the brushite and the remaining TetCP react to form HAp. MCPM is consumed in the first few minutes of reaction, while  $\text{Ca}(\text{OH})_2$  (if present) is still detected after 5–10 min of reaction. After this time of reaction, the brushite formed as a result of MCPM incongruent dissolution reacts with TetCP under invariant conditions to form HAp. The kinetics of the reactions correlate with the variations of the reactants in the aqueous phase. The total heats of reaction were found to be compositionally dependent; however, the overall kinetic behaviour was independent of the initial proportions of the reactants. Isothermal calorimetry shows a period of significant heat evolution occurs during the first 15 min after mixing. After this period, the subsequent rate of reaction becomes slow, and unreacted brushite and TetCP can be detected after 24 h of reaction in slurries of high solids content. The slow reactions identified in this study are severally similar to those observed involving monetite and TetCP.

#### Acknowledgements

The authors gratefully acknowledge the Air Force Office of Scientific Research, Materials Science Directorate for supporting this investigation. R.I.M. also acknowledges the National Science Foundation, DRM Grant no. 8812824. The Environmental Scanning Electron Microscope used in this study was

acquired with NSF support, which is also gratefully acknowledged.

## References

1. W. VAN BRAEMDONCK, P. DUCHEYNE and P. DEMESTER, in "Metal and ceramic biomaterials", Vol. II, edited by P. Ducheyne and G. W. Hastings (CRC Press, Boca Raton, FL, 1984) p. 144.
2. P. S. EGGLI, W. MULLER and R. K. SCHENK, *Clin. Orthop.* **322** (1988) 127.
3. G. HEIMKE, *Angew. Chem.* **101** (1989) 111.
4. M. E. EL DEEB, P. C. TOMPACH and A. T. MORESTAD, *J. Oral Maxillofac. Surg.* **46** (1988) 955.
5. N. HOSAKA and T. NAGATA, *ibid.* **45** (1987) 583.
6. J. F. KAY, M. JARCO, G. LOGAN and S. T. LIU, *Trans. Soc. Biomater.* **9** (1986) 13.
7. S. D. COOK, K. A. THOMAS, J. F. KAY and M. JARCO, *Clin. Orthop.* **232** (1988) 225.
8. A. L. BOSKEY and A. S. POSNER, *J. Phys. Chem.* **80** (1976) 40.
9. E. C. MORENO and K. VARUGHESE, *J. Cryst. Growth* **53** (1981) 20.
10. T. P. FEENSTRA and P. L. DEBRUYN, *J. Phys. Chem.* **84** (1979) 475.
11. L. BRECEVIC and H. FUREDI-MILHOFER, *Calcif. Tissue Res.* **10** (1972) 82.
12. Z. AMJAD, P. KOUTSOUKOS, M. B. TOMSON and G. H. NANCOLLAS, *J. Dent. Res.* **57** (1978) 909.
13. P. KOUTSOUKOS, Z. AMJAD, M. B. TOMSON and G. H. NANCOLLAS, *J. Amer. Chem. Soc.* **102** (1980) 1553.
14. W. E. BROWN and L. C. CHOW, in "Cements research progress-1986", edited by P. W. Brown (American Ceramic Society, Westerville, OH, 1987) pp. 351-377.
15. A. KAPLAN and L. L. SAZBO, in "Clinical chemistry" (Lea and Febiger, Philadelphia, PA, 1983) p. 94.
16. F. C. M. DRIESSENS, in "Bioceramics of calcium phosphates", edited by K. de Groot (CRC Press, Boca Raton, FL, 1983) p. 1.
17. P. W. BROWN and M. FULMER, "Kinetics of hydroxyapatite formation at low temperature", *J. Amer. Ceram. Soc.* **74** (1991) 934-940.
18. P. W. BROWN, N. HOCKER and S. HOYLE, *ibid.* (1991), in press.
19. K. L. ELMORE and T. D. FARR, *Ind. Engr. Chem.* **32** (1940) 580-586.
20. P. T. CHENG, *Calcif. Tissue Int.* **40** (1987) 9-43.
21. B. B. TOMAZIC, M. S. CHUNG, T. M. GREGORY and W. E. BROWN, *Scanning Micro.* **3** (1988) 119-127.
22. N. EIDLEMAN, L. C. CHOW and W. E. BROWN, *Calcif. Tissue Int.* **40** (1987) 71.

Received 4 January  
and accepted 18 June 1991